Phase Behavior and Viscoelasticity of AOT Microemulsions Containing Triblock Copolymers

U. Batra[†] and W. B. Russel*

Department of Chemical Engineering, Princeton University, Princeton, New Jersey 08544-5263

M. Pitsikalis, S. Sioula, and J. W. Mays

Department of Chemistry, University of Alabama at Birmingham, Birmingham, Alabama 35294

J. S. Huang

Exxon Research and Engineering Co., Annandale, New Jersey 08801

Received April 4, 1997; Revised Manuscript Received July 28, 1997[⊗]

ABSTRACT: Mixtures of AOT (sodium bis(2-ethylhexyl) sulfosuccinate)/water/decane microemulsions with polyethylene oxide/polyisoprene/polyethylene oxide (PEO/PI/PEO) triblock copolymers form highly associated solutions with unusual phase behavior and concentration dependence of the viscoelastic moduli. A gas−liquid phase transition, reported here for the first time in these mixtures, is attributed to the entropic gain accompanying the conversion of loops to bridges, in accord with theories for polymer brushes. The homogeneous condensed phase is highly viscous and elastic. The volume fraction dependence of the high-frequency modulus conforms to expectations from theories for either reversible networks or solutions of flowerlike micelles. The apparent low shear, or plateau, viscosity, on the other hand, exhibits a maximum at a volume fraction roughly twice that at the phase boundary. This unusual behavior is predicted qualitatively for solutions of flowerlike micelles, but the quantitative aspects of the response are more difficult to rationalize.

Introduction

Associative polymers are a widely exploited class of additives for tuning the rheology of dispersions.[1−4] Numerous investigators have studied the rheology and phase behavior of the simplest and most successful aqueous associating systems, linear chains with terminal stickers.[5−9] The typical viscosity profile consists of three regimes: (1) Newtonian at low shear rates, (2) shear thickening at moderate shear rates, and (3) shear thinning at high shear rates. The Newtonian plateau at low shear indicates the lack of a yield stress, which implies that the associations are constantly breaking and forming by Brownian motion.

The combination of triblock copolymers having hydrophilic end blocks with AOT (sodium bis(2-ethylhexyl) sulfosuccinate)/water/isooctane microemulsions of droplet radius R_d generates reversible networks due to association of the end blocks with the water cores and the formation of bridges between droplets.[10−18] Triblocks consisting of poly(oxyethylene) (PEO) end blocks and 3,4-poly(isoprene) (PI) mid blocks form fluids with a high low-shear viscosity, while some telechelic ionomers with the same mid block but terminal groups of a sodium salt of sulfonic acid give much weaker associations and much lower relative viscosities.[14] Since the PEO end blocks are soluble only in water and the PI mid blocks only in the alkane, these polymers do not dissolve in the pure solvents, so the aggregation numbers are determined stoichiometrically.

In this paper we report some unusual aspects of these systems, uncovered in the process of exploring the dependence of the viscoelasticity on the molecular weight and composition of the triblock, the overall concentration of polymer plus AOT droplets, and the aggregation number. Since the polymers are insoluble in decane alone, high dilutions must produce flowerlike micelles with the PEO chains in the water core of the AOT droplets and the PI chains forming a corona of loops. As the concentration increases the micelles begin to interact and eventually produce a gas−liquid transition. This phase transition is apparently the consequence of the entropic gain in free energy due to exchange of terminal blocks between the aqueous cores of interacting micelles.[19] In the condensed liquid phase, at fixed polymer to droplet ratio, the shear modulus increases monotonically with concentration, but the low shear/low frequency plateau in the viscosity passes through a maximum at roughly twice the concentration at the phase boundary and then falls substantially for each of our samples.

Associated polymer solutions generally are expected to conform to the classic reversible network theory, with elaborations to account for chains that do not contribute to the elastic network.[9] This approach ignores excluded volume interactions and presumes junctions of relatively low functionality. The gas−liquid phase transition and the maximum in the viscosity lie beyond the scope of the reversible network theory but are predicted qualitatively by Semenov et al.,[19] on the presumption of strong excluded volume interactions between flowerlike micelles with high aggregation numbers. In the following sections we report results for three different formulations, complemented by another from the literature, and compare qualitatively with predictions from both theories.

Background

Eicke and co-workers[10−18] studied five different PEO/PI/PEO triblocks in AOT/water /isooctane (Table 1) for

[†] Present address: Merck & Company, Inc., M-M-R II Technology, West Point, PA 19486.

[⊗] Abstract published in *Advance ACS Abstracts,* September 1, 1997.

S0024-9297(97)00465-8 CCC: $14.00

Table 1. Polymers Employed by Eicke et al.[10−18] to Investigate the Structure and Rheology of Reversible Networks in AOT/Water/Isooctane at $X = 60$

polymer	COP1	COP2	COP3	COP4	COP5
M_{PEO} (kg/mol)	1.7	6.5	11	3.25	6.5
M_{PI} (kg/mol)	85.3	61.5	39	19.5	16.0
S_{PI} (nm)	23.7	20.1	16	11.3	10.3

a molar ratio of water to surfactant of $X \sim 60$, such that $R_d \approx 12$ nm and $S/R_d = 1-2$, where S is the end-to-end distance of the mid block (Table 1). Such a mixture can be diluted in two straightforward ways: (1) adding microemulsion of the same concentration, thereby decreasing the number of polymers per droplet while keeping the mean distance between droplets fixed, or (2) adding solvent, thereby increasing the mean interdroplet distance while maintaining the number of polymers per droplet. Through these dilutions the transition between fluid and gel phases and the volume fraction dependence of the low-shear viscosity and high-frequency modulus in the fluid phase were characterized. Dilution with microemulsion leads to a highly nonlinear but monotonic and reasonably normal decrease in viscosity. Nonetheless, the data appear to be specific to the individual triblock and microemulsion compositions, providing no sense of the parametric dependence on molecular weight and structure or number of polymers per droplet. Therefore, the ability to generate highly viscous systems is clear, but tuning of the response through the molecular structure is still not possible.

Since straightforward formulation produces desirable rheological properties, e.g. high low-shear viscosity and shear thinning, AOT microemulsions containing associative triblocks should serve as convenient models for understanding the interactions and rheology of associated fluids, including those containing particles. However, isooctane, with a flash point around room temperature, is an awkward solvent. Therefore, we explore the rheology with decane as the continuous phase and vary the composition and concentration of the PEO/PI/PEO triblocks. These associative mixtures fall between permanently cross-linked networks and normal polymer solutions, with binding of their terminal groups providing a reversible cross-link.[20−22] Upon dilution with decane we generally encounter a phase separation, indicating that solvent swells the network to only a limited extent, eventually separating excess solvent and some polymer into a dilute, low viscosity solution.[23] While Zolzer and Eicke[14] report no such phase separation, Semenov et al.[19] predict a comparable gas−liquid transition, reflecting the balance between a gain in free energy of $O(kT)$ per chain bridging between interacting micelles and the resulting loss in translational entropy of the micelles.

Linear viscoelastic measurements probing the dynamics of associating polymer solutions generally detect a response characterized by a single relaxation time τ and low-shear viscosity η_o.[9] The shear and loss moduli, G' and G'', then vary with frequency as

$$G' = G'_\infty \frac{(\omega\tau)^2}{1+(\omega\tau)^2} \qquad G'' = \eta_o \frac{\omega}{1+(\omega\tau)^2} \tag{1}$$

with $G'_\infty = \eta_o/\tau$. These small amplitude oscillatory measurements differentiate between solids and liquids on the basis of the behavior of G' at low frequencies. For a solid $\tau \to \infty$ so that $G' = G'_\infty$ for all frequencies,

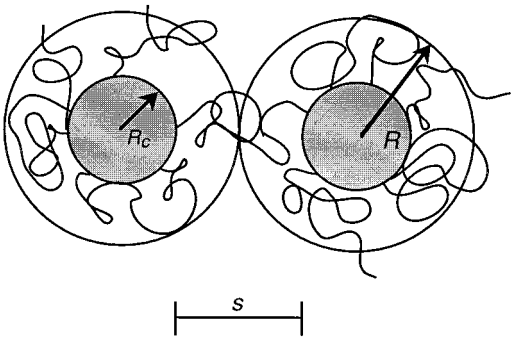

Figure 1. Associated microemulsion with droplets of radius R_d decorated with copolymers having mid block with end-to-end distance S forming spherical entity of radius R.

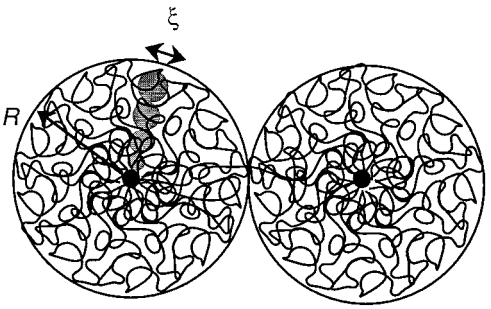

Figure 2. Flowerlike micelles of Semenov et al.[19] illustrating radius R and blob size ξ with p polymers per micelle.

but for a fluid $G' \approx G'_\infty$ only as $\omega \to \infty$. At low frequencies the stresses relax toward zero with $G' \approx G'_\infty(\omega\tau)^2$ and $G'' \approx \eta_o\omega$. Either of two time scales control the dynamics of micellar solutions of associative polymers: τ_b for end block disengagement[9] or τ_d for droplet diffusion or hopping[19]

$$\tau_b = \frac{S^2}{D_p}\exp(N_o + \chi) \tag{2}$$

$$\tau_d = \frac{R^2}{D}\exp\left(N_o + \frac{VG'_\infty}{kT}\right)$$

Here R is the radius of the micelles, D_p and D are the Stokes-Einstein diffusion coefficients for the mid block and the micelle, respectively, N_o is the number of bridging chains per micelle, V is the volume of a micelle, and χ is the exchange energy of the end block between the water cores and decane normalized by kT. In either case a droplet must escape the attractive minimum in the pair potential due to bridging chains, hence the Boltzmann factor $\exp(N_o)$. Full relaxation of the bridges also depends on the energy barrier χkT associated with the end block passing through the continuous phase, while diffusion or hopping of the micelle requires the creation of a site at the expense of VG'_∞ in elastic energy.

Semenov et al.[19] consider telechelic polymers (with long mid blocks and short end blocks or stickers) that aggregate to form flowerlike micelles (Figure 2) to consist of a compact core surrounded by a corona of long soluble mid blocks that form loops. The micelle, therefore, resembles a star polymer with a functionality p (number of chains per micelle) that depends on the energy of interaction between the stickers and the molecular weight of the chain. For micelles with very large functionalities ($p \approx 30-100$) the corona of loops behaves as a polymer brush.[24−26] The interaction between two such micelles produces a bridging attrac-

tion at a separation of $2R_o$, where R_o is the radius of an isolated micelle, and a repulsive interaction as the brushes are compressed at smaller separations. The attractive interaction is proportional to the number of bridges N_o with the minimum occurring at the "classical contact" between coronas, i.e. at a separation of $R_o - \xi_o$ with $\xi_o \approx lN^{\nu}p^{-\nu/6}$ being the blob size at the edge of the layer and $R_o \approx lN^{\nu}p^{(1-\nu)/2}$ ($\nu = {}^3/_5$ for good solvents) being the radius of an isolated micelle. The number of bridges is roughly the number of chains per unit area times the area of contact, $N_o \approx \xi_o R_o \times \xi_o^{-2} = R_o/\xi_o$, so the attractive minimum is $O(p^{(3-2\nu)/6})$. The corresponding second virial coefficient in the osmotic pressure of the micellar solution

$$B_2 \approx \frac{2\pi}{3} R_o^3 [1 - 3p^{(2\nu-3)/6} \exp(p^{(3-2\nu)/6})] \qquad (3)$$

is negative for any p, though this approximation is asymptotically valid only for $p \gg 1$. The spinodal associated with a gas−liquid binodal occurs when the osmotic compressibility vanishes, implying phase separation for number densities of micelles greater than $(2B_2)^{-1}$, which decreases with increasing p. The authors presumed the dense phase to be volume filling, i.e. with volume fraction $\phi = 4\pi R_o^3 n_p/3p \approx 1$ and n_p the number density of chains.

Through an extension of these arguments Semenov et al. also obtaining scaling relations for the shear modulus as a function of the volume fraction ϕ as

$$\frac{R_o^3 G'_\infty}{kT} \approx p^{3/2}(\phi - 1)^{6\nu/(3-2\nu)} \qquad (4)$$

for $\phi - 1 \ll 1$ and

$$\frac{R_o^3 G'_\infty}{kT} \approx p^{3/2}\left(\frac{\phi}{2}\right)^{(3\nu-4/3)/(3\nu-1)} \qquad (5)$$

for $\phi - 1 = O(1)$ (Figure 3a). They argue that for $p \gg 1$ the elastic stress and, therefore, the concentration dependence of the elastic modulus arise from the compression of close-packed micelles, with the bridges merely providing the attraction to assemble the condensed phase.

The relaxation time for micellar diffusion or hopping follows directly from (eq 2) with the volume of the micelle depending on concentration as $V = 4\pi R_o^3/3\phi$. They then estimate the low-shear viscosity from the modulus and relaxation times as

$$\eta_o = G'_\infty \max(\tau_d, \tau_b) \qquad (6)$$

The qualitative nature of the volume fraction dependence of the viscosity depends on the relative rates of the two modes of relaxation. If $\chi > p^{3/2}$, the end block disengagement (or relaxation of bridges) controls and the viscosity increases monotonically from the phase boundary. If $\chi < p^{3/2}$ the micellar diffusion process is slower and the viscosity increases for $1 < \phi < 2$ but then decreases for $\phi > 2$ (Figure 3b). The latter behavior arises from the contraction of the chains in the corona with increasing concentration, which outweighs the modest rate of increase of the shear modulus for $\phi > 2$ and causes the hopping energy to decrease with increasing ϕ. The theory predicts the viscosity at $\phi = 2$, which is a maximum for $\chi < p^{3/2}$, to depend only on p and χ as

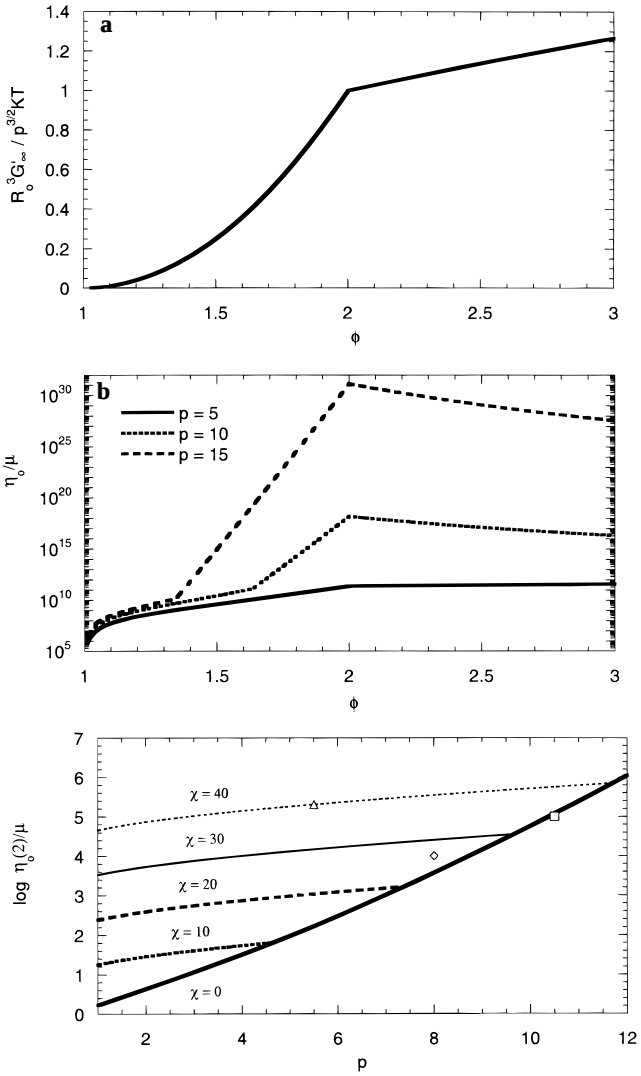

Figure 3. Predictions from theory of Semenov et al.[23] for (a) the normalized high frequency modulus for all p and χ, (b) the low-shear viscosity as a function of p for $\chi = 20$, and (c) the value predicted for the low-shear viscosity at $\phi = 2$ for several values of χ with compared with maximum values for the plateau viscosity estimated from data for JM2 with $p = 10.5$ (□), JM2 with $p = 8$ (◇), and JM3 with $p = 5.5$ (△). For (c) the predicted value of $\log(\eta_o(2)/\mu)$ has been multiplied by 3/11 to match the measured magnitudes.

$$\frac{\eta_o(2)}{\mu} \approx p^{3/2} \exp\{p^{5/6} + \max(\chi, p^{3/2})\}$$

with μ the solvent viscosity. This produces a family of curves for different χ, merging into a single curve for $\chi < p^{3/2}$ (Figure 3c). Note that the viscosities predicted are unrealistically large, perhaps due to the omission of prefactors in the theory.

In this paper we report observations of phase separation and viscoelasticity for three mixtures of PEO/PI/PEO triblocks with AOT/water/decane microemulsions. Since each exhibits a gas−liquid transition and a maximum in the viscosity, we draw on the Semenov theory to correlate and interpret the results.

Experimental Procedures

Polymer Synthesis. We synthesized narrow molecular weight distribution (Table 2) PEO/PI/PEO triblocks with a range of mid block and end block sizes. The synthesis of these particular triblocks is unusual and nontrivial, so the methods are described in detail here.

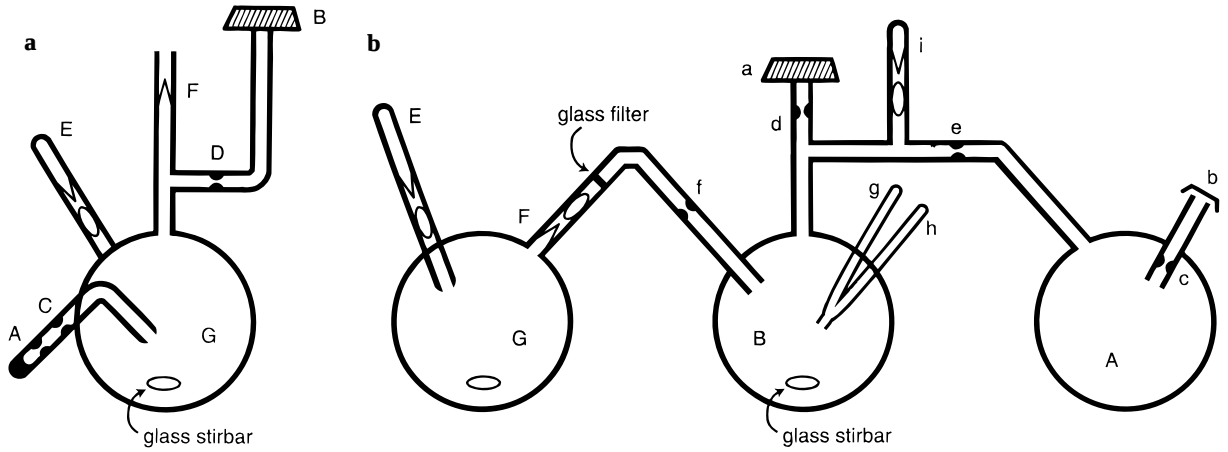

Figure 4. Apparatus for anionic synthesis of the triblock copolymers: (a) for preparation of potassium/naphthalene initiator; (b) for polymerization.

Table 2. Specifications for Polymers

	polymer	$M_{PEO}/2$ (kg/mol)	S_{PEO} (nm)	M_{PI} (kg/mol)	S_{PI} (nm)	M_w/M_n
JM2	PEO/PI/PEO	2.2	1.5	21.3	11.8	1.06
JM3	PEO/PI/PEO	7.9	2.8	55.8	19.1	1.08

Tetrahydrofuran (THF, Fisher Scientific) was refluxed over Na for 3 h and then distilled over Na/K alloy on the vacuum line. Naphthalene (Aldrich) was vacuum sublimed three times in a special apparatus and diluted in vacuo with hexane. The concentration of naphthalene was determined by measuring the molecular weight of a polystyrene prepared by polymerizing a known amount of purified styrene with a K/naphthalene initiator prepared by reacting a measured volume of naphthalene/hexane with excess K mirror (described below). Isoprene (Aldrich) was purified by sequential exposure to and distillation from CaH_2 (overnight), Na dispersion (1 h, 0 °C), and *n*-BuLi (twice for *ca.* 1 h, 0 °C). The monomer was then diluted under vacuum with THF to give a 20% monomer solution. Ethylene oxide (EO, Kodak) was dried over CaH_2 and then distilled three times over *n*-BuLi (*ca.* 1 h at 0 °C each time).

The apparatus for producing the K mirror (Figure 4a) holds a small quantity of K in the side arm (A) under an inert atmosphere. The tube was sealed and the apparatus was attached to the vacuum line through a ground joint (B). After pumping the apparatus to $<10^{-5}$ mmHg, the side arm was gently heated with a torch, distilling metal into the flask and forming the mirror. After a sufficient quantity of K had been distilled, the side arm was removed by sealing at the constriction (C). THF was distilled into the apparatus and the flask was sealed at constriction D and removed from the vacuum line. This flask (G), which was equipped with a naphthalene ampule (E) and breakseal (F), was then was used in the polymerization as described below.

The polymerization apparatus (Figure 4b) consists of the flask (G) with the K mirror connected to the polymerization apparatus through breakseal F. The reactor was attached to the vacuum line through ground joint a and pumped down. A small amount of *n*-BuLi was injected into flask (A) through the septum (b), and the side arm was removed by sealing at constriction c. Purified benzene was distilled into flask A and the reactor was removed from the vacuum line by sealing at constriction d. Using the benzene solution of *n*-BuLi, the entire apparatus was purged and then rinsed by condensing benzene onto the walls of the apparatus (taking ca. 2 h). The benzene and *n*-BuLi were finally collected in flask A and this "purge section" was removed by sealing at constriction e. The breakseal to the naphthalene ampule (E) was then broken, and the naphthalene reacted with the K mirror to form the initiator. A deep green color immediately formed and the reaction was allowed to continue over 2 h at 5−10 °C with continuous stirring. The breakseal (F) was then ruptured and the initiator solution was transferred from flask G to flask B; flask G was then removed by heat sealing at constriction f. The K/naphthalene solution was cooled in a dry ice/isopropyl alcohol bath and stirred rapidly with a glass stirrer. After the isoprene ampule was chilled, the breakseal g was broken and a yellow-orange color (depending on the concentration of living chain ends) immediately developed. The reaction proceeded at −78 °C for 1 h. The EO ampule (h) was then chilled, and the breakseal was broken. The solution became extremely viscous and the apparatus was warmed to room temperature. Gradually, the color disappeared, and when the solution was completely colorless, the flask was placed in a water bath at 50 °C for 5 days. The polymerization was then terminated by introduction of methanol from ampule i. After concentration on a rotary evaporator, the polymer was precipitated into water/methanol or pure water (depending on the polymer) containing a small amount of stabilizer (butylated hydroxytoluene, BHT).

Table 3. Comparison of Volume Fractions at the Onset of the Phase Separation ϕ_d* with the Prediction from Equation 8

				ϕ_d*	
polymer	p	N_{PEO}	$p^{3/2}$	eq 8	exptl
COP3	22	66	103	0.074	
JM2	10.5	13	34	0.046	0.088
JM2	8	13	23	0.052	0.09
JM3	5.5	33	13	0.018	0.039

300 MHZ ^{1}H-NMR was used to determine the composition of the block copolymers and the microstructure of the PI (ca. 80% 3,4 with the remainder mostly 1,2). The polydispersities of the copolymers were determined with size exclusion chromatography (SEC) in THF. The samples for this work exhibited narrow, monomodal molecular weight distributions characterized by weight- (M_w) to number-average (M_n) molecular weights of 1.06−1.08 (Table 3). The absolute M_ns were measured via membrane osmometry (Jupiter Instruments Company) in toluene at 37 °C.

Sample Preparation. The microemulsion is formulated by mixing dry, redistilled AOT with water and decane such that the molar ratio of water to AOT equals $X = 40.8$. The volume fraction, ϕ_d, of the droplets is calculated from the formulation as

$$\phi_d = \frac{c_{H_2O}}{\rho_{H_2O}} + \frac{c_{AOT}}{\rho_{AOT}}$$

The hydrodynamic radius, measured by dynamic light scattering as 6.6 nm, exceeds slightly the droplet radius expected from the linear relationship $R_d = 0.70 + 0.136X$ (nm) for $X = 40.8$. Since the copolymers do not dissolve directly in decane, the solutions were prepared by adding polymer to a microemulsion at ϕ_d such that S_{PI} exceeds the mean distance

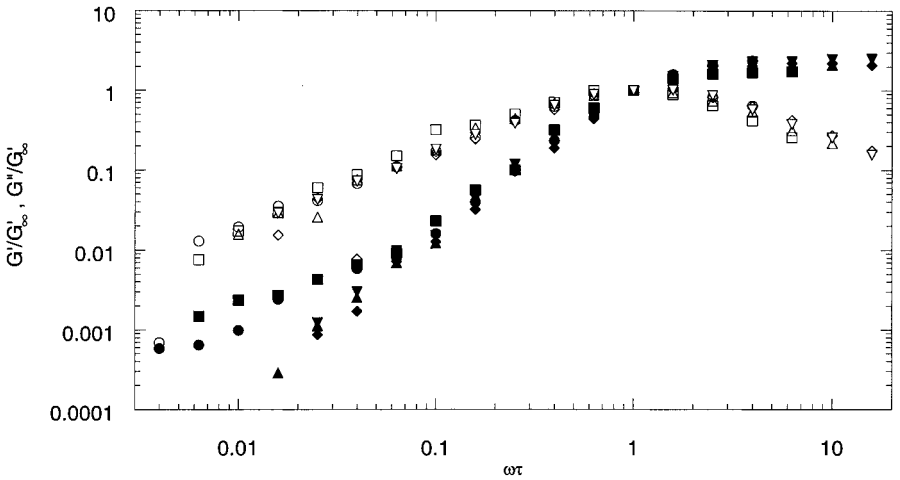

Figure 5. Superposition of the viscoelastic spectra for data from JM3 with $p = 5.5$ at $\phi_d = 0.049$ (▽), 0.054 (△), 0.060 (◇), 0.080 (□), and 0.100 (○): filled symbols, G'; open symbols, G''.

between of two droplets. This should allow a mid block to bridge between neighboring droplets and form an infinite network without stretching. Between 30 and 60 days are required to fully solvate the solutions. At large $p = n_p/n_d$ (number of polymers per droplet) the solution becomes extremely viscous and the dissolution requires very long times. Thus we selected the maximum number of polymers per droplet such that dissolution times are reasonable.

Rheology. Rheological measurements were performed on a Rheometrics RFS2 rheometer with a cone and plate of 50 mm diameter, a 0.04 radian cone angle, and a 1 mm gap at the edge of the plate. To ensure reproducibility, the samples are loaded without entraining air and evaporation is retarded effectively by placing solvent-soaked Kimwipes in the environmental chamber. A steady shear experiment applies a constant strain rate and detects the resulting shear stress to determine the steady shear viscosity. High viscosity samples take between 10 and 60 s to reach steady state, so each sample was run with increasing and decreasing shear rates over the range 2.5×10^{-2} to 10^2 s^{-1}, unless limited by the torque, to confirm the absence of hysteresis.

Our oscillatory experiments first established the range of strains that produce a linear response and then stepped through the frequency range at a rate that permitted equilibration at each step. The resulting data for G' and G'' as a function of frequency invariably displayed a fluid response dominated by a dominant relaxation time over the accessible range of frequencies, 10^{-1}−10^2 Hz. Only for the higher concentrations did a weaker, second relaxation emerge at low frequencies, so we fit the data to a Maxwell model to extract the apparent low-shear viscosity η_{pl} and high frequency modulus G'_∞. The success of this approach is demonstrated via the superposition of the data at all concentrations for one of the three formulations studied in Figure 5. The dependence of G'_∞ and η_{pl} on concentration and the other parameters of the formulation is discussed below. Values of η_{pl} extracted from G'' are consistent with those detected in steady shear. Nonetheless, we refer to the former as the plateau viscosity associated with the observed relaxation, due to lingering uncertainty about the existence of a second relaxation at much lower frequencies.

Results and Discussion

Phase Behavior. Even though batch solutions can be diluted with microemulsion at the same ϕ_d to $n_p = 0$, dilution with pure solvent results in a phase separation.[27] The lower phase consists of a hazy high-viscosity fluid, which clears in 5−10 days, while the upper phase is a clear low-viscosity fluid. Preliminary dynamic light scattering measurements on the latter indicate a dilute solution of droplets with some polymer ($R_o \approx 10$ nm). The phase transition occurs in all three systems with the estimated composition at the phase boundary listed in Table 3. Zolzer and Eicke[14] report no such phase transition when diluting COP3 and AOT/water/isooctane microemulsions with solvent, but Thibeault et al.[23] report a similar transition in aqueous solutions of poly(oxyethylene) end capped with C_{14}−C_{18} hydrophobes.

To apply the theory for micelles to microemulsions we adopt the Daoud−Cotton model,[28] which envisions the polymer layer as consisting of blobs of dimension ξ containing N_ξ segments with $\xi \approx lN_\xi^{3/5}$. Each spherical shell of radius $R_d < r < R_o$ concentric with the droplet comprises a close packed layer of blobs dictating that $4\pi r^2 = p\xi^2$. Integrating the segment density N_ξ/ξ^3 across the layer and setting the total number of segments to pN determines the size of the composite droplet as

$$R_o = R_d\left\{1 + 0.72p^{1/3}\left(\frac{S}{R_d}\right)^{5/3}\right\}^{3/5} \qquad (7)$$

The theory then stipulates the volume fraction of droplets in the condensed phase to be

$$\phi_d^* \approx \left(\frac{R_d}{R_o}\right)^3 = \left\{1 + 0.72p^{1/3}\left(\frac{S}{R_d}\right)^{5/3}\right\}^{-9/5} \qquad (8)$$

The values in Table 4 indicate this to be roughly correct. Thus, the phase transition appears to be as described by Semenov et al.[19]

Linear Viscoelasticity. Table 4 displays G'_∞ as a function of n_p, the number density of polymer chains, for our three systems plus COP3 of Eicke et al. with the error estimates reflecting the uncertainty in fitting to the Maxwell model. In all cases, the modulus, which is insensitive to temperature, rises essentially monotonically with increasing number density. Clearly, though, the modulus also depends on the other parameters of the formulation, i.e., the size and volume fraction of the AOT droplets and molecular weight and asymmetry of the triblock. To better correlate these measurements we scale the modulus both as G'_∞/n_pkT in accord with expectations from reversible network theories (Figure 6, open symbols) and as $4\pi R_o^3 G'_\infty/p^{3/2}kT$ to conform to eqs 4 and 5 from the Semenov theory (Figure 6, closed symbols) and plot them as a function of $\phi = \phi_d/\phi_d^*$. For COP3 we take $\phi_d^* = 0.156$ to bring that data in line with the rest. The reduced modulus

Table 4. Concentration Dependence of High-Frequency Modulus and Low-Shear Viscosity for Data from Batra[27] and Eicke et al.[10−18]

JM2; $p = 10.5$ H_2O/AOT/decane			JM2; $p = 8$ H_2O/AOT/decane			JM3; $p = 5.5$ H_2O/AOT /decane			COP3; $p = 22$ H_2O/AOT/isooctane		
ϕ_d	G'_∞ (Pa)	η_{pl}/μ	ϕ_d	G'_∞ (Pa)	η_{pl}/μ	ϕ_d	G'_∞ (Pa)	η_{pl}/μ	ϕ_d	G'_∞ (Pa)	η_{pl}/μ
0.10	1210 ± 350	1.18×10^4	0.117	2400 ± 600	6.74×10^3	0.049	440 ± 180	6.42×10^4	0.083	130 ± 80	5.1×10^3
0.12	4220 ± 1800	1.69×10^4	0.128	3010 ± 1200	7.33×10^3	0.054	830 ± 320	8.51×10^4	0.170	800 ± 300	4.11×10^4
0.14	7880 ± 3600	2.96×10^4	0.149	6020 ± 2800	9.81×10^3	0.060	1410 ± 600	1.89×10^5	0.179	1200 ± 400	1.98×10^5
0.16	7520 ± 1520	1.01×10^5			1.67×10^3	0.080	2640 ± 1200	2.14×10^5	0.259	5300 ± 2800	1.33×10^6
0.18	7830 ± 1550	5.91×10^4				0.100	3340 ± 1200	1.18×10^5			
0.20	620 ± 4000	2.36×10^4									

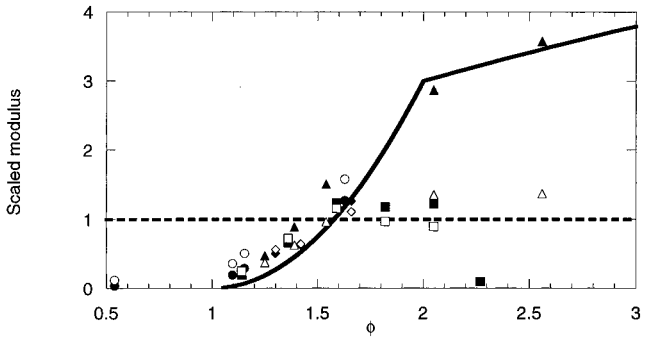

Figure 6. High-frequency shear modulus scaled on both n_pkT (open symbols) and $3p^{3/2}kT/4\pi R_o^3$ (filled symbols) and plotted against $\phi = \phi_d/\phi^*_d$: COP3 with $p = 22$ (○), JM2 with $p = 10.5$ (□), JM2 with $p = 8$ (◇), JM3 with $p = 5.5$ (△), and $G'_\infty/n_pkT = 1$ (- - -), and $4\pi R_o^3 G'_\infty/9p^{3/2}kT$ from eqs 4 and 5.

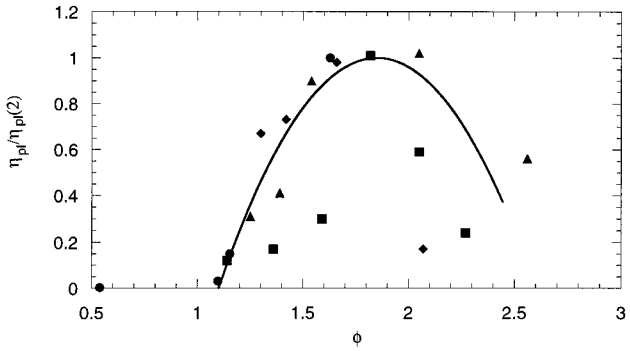

Figure 7. Plateau viscosity normalized on the maximum value for COP3 with $p = 22$ (○), JM2 with $p = 10.5$ (□), JM2 with $p = 8$ (◇), and JM3 with $p = 5.5$ (△). The curve is drawn to guide the eye.

is order one and the superposition is reasonable with both scalings.

The theoretical curve from eqs 4 and 5, which omits all numerical prefactors, conforms to the data to some degree. Furthermore, the transition from weak to strong compression roughly correlates the change in slope of the experimental data for $\phi > 2.0$. This limited success implies that the elastic response of the mixture, indeed, might arise from the compression of the chains surrounding the microemulsion droplets rather than from the stretching of bridges as assumed in conventional transient network theories. Reinforcing this speculation is the fact that $G'_\infty/n_pkT > 1$ for some of the open symbols, which is generally not expected in the reversible network theory in the absence of entanglements.

Shear Viscosity. Although dilution of JM2 in AOT/water/decane with microemulsion at fixed ϕ_d decreases the viscosity monotonically to the value for the neat microemulsion,[27] dilution from the same starting point with pure solvent first increases the viscosity, e.g., for JM2 at $p = 10.5$ from $\eta_{pl}/\mu \approx 2.4 \times 10^4$ at $\phi_d \approx 0.20$ to $\eta_{pl}/\mu \approx 1 \times 10^5$ at $\phi_d \approx 0.16$ (Table 4). Upon further dilution the viscosity falls by 1−2 orders of magnitude before the solution phase separates. Normalizing all three sets of data on the maximum viscosity (Figure 7) illustrates the similarity among the three systems, though the magnitudes vary substantially. To our knowledge, only one other, rather sketchy, report[29] exists of a viscosity maximum upon dilution of associative polymer solutions. Zolzer and Eicke[14] report a monotonically decreasing viscosity upon dilution of COP-3 in AOT/water/isooctane with solvent. Our rescaling of their data suggests that a maximum might appear at a somewhat higher concentration.

Though the variation of the viscosity with concentration resembles that predicted by the Semenov theory in Figure 3b, quantitative comparison is difficult due to the extreme sensitivity of theory to p and ϕ and the absence of numerical prefactors in the exponentials. The qualitative form of the normalized viscosities is suggestive but difficult to interpret. The primary point of contact between the theory and our data is the existence of a maximum in the viscosity, for which their explanation in terms of an elastic energy that decreases with volume fraction for $\phi > 2$ is the only one currently available. However, the p-dependence of the maximum viscosity (Figure 3c) does not conform to expectations for the $\chi > p^{3/2}$ regime indicated by the lowest curve.

Constructing a dimensionless relaxation time for each mixture as $\bar{\tau} \equiv \eta_{pl}kT/\mu R_o^3 G'_\infty$ and evaluating it from the data at $\phi = 1.7-2.0$ reveals interesting variations:

$$\bar{\tau} = 1600 \quad \text{COP3} \quad p = 22$$

$$500 \quad \text{JM2} \quad p = 10.5$$

$$100 \quad \text{JM2} \quad p = 8$$

$$1500 \quad \text{JM3} \quad p = 5.5$$

This nonmonotonic variation with decreasing p might suggest a different mechanism for the last formulation, JM3 with $p = 5.5$. Returning to the plot of log $(\eta_o(2)/\mu)$ vs p (Figure 3c) and recognizing that the data points correspond to different values of χ imply that they should correspond to different parametric curves if $\chi > p^{3/2}$. Suppose that $\chi = \chi_o N_{PEO}$ with $0.4 < \chi_o < 1.6$, then the COP3 and the two JM2 mixtures would satisfy $\chi < p^{3/2}$, while the JM3 mixture would have $\chi > p^{3/2}$. In this circumstance the theory would attribute the relaxation of JM3 to disengagement of the end block from the core of the droplet, with a viscosity at $\phi = 2.0$ corresponding to one of the curves on the left hand side of the plot. Both JM2 samples and COP3 would still be controlled by the relaxation time for elastic hopping. Of course, this ignores the very large difference in magnitude between the predictions and the measurements and the fact that JM3 also exhibits the maximum in the viscosity, which the theory does not predict for $\chi > p^{3/2}$.

Conclusions

Associated solutions, constituted of AOT microemulsions and PEO/PI/PEO triblock copolymers, diluted with decane display some interesting properties: below $\phi_d \approx O(R_d/R_o)^3$ the solution phase separates into a clear, low viscosity phase and an initially turbid, high viscosity phase; G'_∞ falls gradually at first but eventually drops rapidly to the phase boundary; and η_{pl}/μ passes through a maximum and then decreases by one or two orders magnitude to the value at the phase boundary.

The mechanism for the dependence of η_{pl}/μ and G'_∞ on p and ϕ remains to be established. Our data conform to some degree with the predictions of Semenov et al.[19] for $p \gg 1$, but a more systematic study is needed to determine the full extent of correlation.

Acknowledgment. This work was supported by a fellowship from Merck Manufacturing to U.B. and the Princeton Center for Complex Materials through the NSF MRSEC Program under Grant No. DMR-9400362.

Nomenclature

B_2	second virial coefficient in osmotic pressure
c	mass concentrations
D	Stokes−Einstein diffusion coefficient of the droplet
D_p	Stokes−Einstein diffusion coefficient of the mid block
G',G''	storage and loss moduli
G'_∞	high frequency shear modulus
kT	thermal energy
l	length of a statistical segment
M_{PEO}	number average molecular weight of the PEO end blocks
M_{PI}	number average molecular weight of the PI mid block
M_w/M_n	polydispersity ratio
n_p	number density of polymer chains
n_d	number density of droplets
N	number of statistical segments per chain
N_o	number of bridging chains between two micelles or droplets
p	functionality of micelle or n_p/n_d
R,R_o	radius of micelle or droplet plus corona and value at infinite dilution
R_d	hydrodynamic radius of the droplet
S_{PI}, S_{PEO}	end to end distance of the PI mid block and PEO end block
V	volume of micelle or droplet plus corona
X	molar ratio of water to AOT

Greek Letters

χ	energy barrier for end block exchange from droplet to solvent
ϕ	ϕ_d/ϕ_d^* effective volume fraction of micelles or droplets plus coronas
ϕ_d, ϕ_d^*	volume fraction of droplets and value at phase transition
η_o	low-shear viscosity
η_{pl}	plateau shear viscosity
μ	solvent viscosity
ν	Flory exponent
ξ	blob size
ρ	density
τ	relaxation time
τ_b	time for relaxation via dissociation of bridges
τ_d	time for relaxation via hopping or diffusion of micelles or droplets plus coronas
ω	frequency of oscillations

References and Notes

(1) Schaller, E.; Sperry, P. R. Associative Thickeners. *Handb. Coat. Addit.* **1992**, *2*, 105.
(2) Schwab, F. G. Water Soluble Polymers: Beauty with Performance. *Adv. Chem. Ser.* **1986**, *213*, Chapter 19.
(3) Sperry, P. R.; Thibeault, J. C.; Kostansek, E. C. *Adv. Org. Coat. Sci. Tech.* **1987**, *9*, 1.
(4) Lundberg, D. J.; Ma, Z.; Glass, J. E. *Proc. Polym. Mater. Sci. Eng. Div. ACS* **1990**, *63*, 440.
(5) Lundberg, D. J.; Glass, J. E. *J. Rheol.* **1991**, *35*, 1255.
(6) Jenkins, R. D.; Silebi, C. A.; El-Aasser, M. S. *Polym. Mater. Sci. Eng.* **1989**, *61*, 629.
(7) Santore, M. M.; Russel, W. B.; Prud'homme, R. K. *Macromolecules* **1989**, *22*, 1317.
(8) Jenkins, R. D.; Silebi, C. A.; El-Aasser, M. S. Polymers as Rheological Modifiers. *ACS Symp. Ser.* **1991**, *462*, 222.
(9) Annable, T.; Buscall, R.; Ettelaie, R.; Whittlestone, D. *J. Rheol.* **1993**, *37*, 695.
(10) Eicke, H. F.; Quellet, C.; Xu, G. *Colloids. Surf.* **1989**, *36*, 97.
(11) Quellet, C.; Eicke, H. F.; Xu, G.; Hauger, Y. *Macromolecules* **1990**, *23*, 3347.
(12) Hilfiker, R.; Eicke, H. F.; Steeb, C.; Hofmeier, U. *J. Phys. Chem.* **1991**, *95*, 1478.
(13) Struis, R. P. W. J.; Eicke, H. F. *J. Phys. Chem.* **1991**, *95*, 5989.
(14) Zolzer, U.; Eicke, H. F. *J. Phys. II (Fr.)* **1992**, *2*, 2207.
(15) Zhou, Z.; Hilfiker, R.; Hofmeier, U.; Eicke, H. F. *Prog. Colloid Polym. Sci.* **1992**, *89*, 66.
(16) Eicke, H. F.; Gauthier, M.; Hilfiker, R.; Struis, R. P. W. J.; Xu, G. *J. Phys. Chem.* **1992**, *96*, 5175.
(17) Fleischer, G.; Stieber, F.; Hofmeier, U.; Eicke, H. F. *Langmuir* **1994**, *10*, 1780.
(18) Odenwald, M.; Eicke, H. F.; Meier, W. *Macromolecules* **1995**, *28*, 5069.
(19) Semenov, A. N.; Joanny, J.-F.; Khokhlov, A. R. *Macromolecules* **1995**, *28*, 1066.
(20) Tanaka, F.; Edwards, S. F. *J. Non-Newtonian Fluid Mech.* **1992**, *43*, 247.
(21) Tanaka, F.; Edwards, S. F. *J. Non-Newtonian Fluid Mech.* **1992**, *43*, 273.
(22) Tanaka, F.; Edwards, S. F. *J. Non-Newtonian Fluid Mech.* **1992**, *43*, 284.
(23) Thibeault, J. C.; Lau, W.; Pham, Q. T. T.; Russel, W. B. Manuscript in preparation.
(24) Witten, T. A.; Pincus, P. A. *Macromolecules* **1986**, *19*, 2509.
(25) Witten, T. A. *J. Phys.* **1988**, *49*, 1055.
(26) Milner, S. T.; Witten, T. A. *Macromolecules* **1992**, *25*, 5495.
(27) Batra, U. Structure and Rheology of AOT Microemulsions: Viscosity Anomalies, Fluctuations and Associating Polymers. Ph.D. Dissertation, Princeton University, 1996.
(28) Daoud, M.; Cotton, J. P. *J. Phys. Paris* **1982**, *43*, 531.
(29) Howard, P. R.; Leasure, E. L.; Rosier, S. T.; Schaller, E. J. *J. Coat. Technol.* **1992**, *64*, 87.

MA970465I